Experimental Study of the Effect of Span Loading on Aircraft Wakes

Victor R. Corsiglia,* Vernon J. Rossow,† and Donald L. Ciffone‡
NASA Ames Research Center, Moffett Field, Calif.

Measurements of the rolling moment induced on a wing trailing in the wake 13.6 spans behind a subsonic transport model were made in the NASA-Ames 40-by 80-Foot Wind Tunnel. It was found that the rolling moment induced on the trailing wing was reduced substantially by reshaping the span loading on the generating model. This was accomplished by retracting the outboard trailing edge flaps. It was concluded from wind tunnel and water tow facility flow visualization studies that this flap arrangement redistributes the vorticity shed by the wing along the span to form three vortex pairs that interact to disperse the wake.

Nomenclature

AR = aspect ratio, b^2/S
b = span of wing
c = wing chord
$\bar{c}$ = average chord, S/b
C_l = rolling-moment coefficient, torque/$(\frac{1}{2}\rho U_\infty^2 Sb)$
C_L = lift-coefficient, lift/$(\frac{1}{2}\rho U_\infty^2 S)$
S = wing area
t = time
U_∞ = freestream velocity (aligned with x axis)
x,y = coordinate axes; x is streamwise and y is spanwise
α = angle of attack
Γ = circulation
ρ = air density

Subscripts

f = following model that encounters wake
g = model that generates wake

Introduction

THE trend toward higher air traffic density at airports coupled with the widening range in aircraft size increases the hazard to small aircraft that might encounter a large aircraft's wake vortices. One form of the hazard is an overpowering rolling moment on the encountering aircraft. The Department of Transportation is studying means for locating these vortices in order to direct aircraft away from the vortex wake and to establish safe operating distances. The NASA effort has been directed at reducing the rolling moment on an encountering aircraft to a controllable level. Initial investigations have focused on ways to accomplish this by changing the generating aircraft configuration only sightly in what would be considered a retrofit modification. The investigation reported herein considers a variety of flap configurations on a typical subsonic jet transport to determine the effect on the vortex wake of the span loading changes that are possible with the existing flap system. Other methods for alleviating the vortex wake intensity, such as turbulence injection into the vortex,[1-3] spoilers,[4] and initiation of vortex instabilities by oscillating the wing geometry,[5,6] are not reported here.

The application of span load modification to the present configuration was stimulated by recent theoretical studies.[7,8] These results were confirmed in a later experimental study of the wake of a swept wing in a water tow facility.[9] In the present experiments, the span loadings produced by independently changing the trailing edge flap deflections approximate the span loadings that were found, theoretically, to yield large vortex cores and interactions between multiple vortices. A B747-type transport model was used in the present tests to generate the wake vortices. As the lift on this generating model was varied by changing the angle of attack, the rolling moment on several trailing wings was measured at various vertical and lateral locations in the wake. The technique used here is similar to that of Wentz,[10] Singh et al.,[11] Banta,[12] Iversen et al.,[13] and Dunham.[14] The work of Dunham (carried out concurrently) uses identical generator model and trailing wings. Dunham's rolling-moment experiments differ, however, in that his models are towed through water, and his results extend to greater downstream distances.§

Apparatus and Test Procedure

Wind-Tunnel Setup

Figure 1 shows a schematic diagram of the test installation in the NASA-Ames Research Center 40- by 80-Foot Wind Tunnel. The generator model is centrally located in the inlet and is attached by a single strut through a straingage balance to measure lift. The angle of attack of the generator was set remotely through an actuator and indicator. At 24.4 m (80 ft) downstream of the generator model, a trailing wing was mounted on a single strut which was remotely positioned vertically over a 3.05-m (10-ft) range and laterally over a 4.27-m (14-ft) range. Additional geometric details of the trailing wings are given in Table 1. The wings were attached to a strut through a straingage balance to measure rolling moment. They were constructed of balsa wood to ensure a high-frequency response. The natural frequency of the wing balance combination (31 Hz, model 1) was several times larger than the rolling moment frequencies encountered. The subsonic transport model (Fig. 2), used as the wake generator was equipped with two spanwise segments of triple-slotted trailing edge flaps, capable of providing high lift. Full-span leading edge slats were installed when the trailing edge flaps were deflected.

Rolling-Moment Measurement

The procedure for recording the rolling moment consisted of setting the generator model and wind-tunnel conditions and selecting a lateral and vertical position for the following model. The time-varying rolling-moment signal was recorded

Presented as Paper 75-885 at the AIAA 8th Fluid and Plasma Dynamics Conference, Hartford, Conn., June 16-18, 1975, submitted Aug. 21, 1975; revision received May 17, 1976.

Index categories: Aircraft Aerodynamics (Including Component Aerodynamics); Jets, Wakes, and Viscid-Inviscid Flow Interactions.

*Aerospace Engineer. Member AIAA.
†Staff Scientist. Associate Fellow AIAA.
‡Aerospace Engineer. Member AIAA.

§The water tow facility is owned and operated by Hydronautics, Inc., Laurel, Md., under contract to NASA-Langley Research Center.

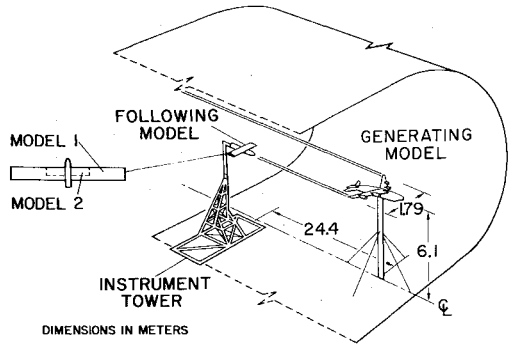

Fig. 1 Experimental setup in the NASA-Ames 40- by 80-Foot Wind Tunnel.

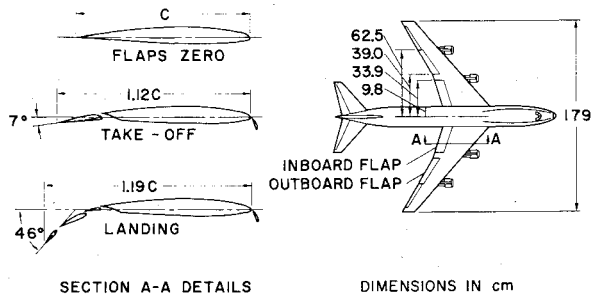

Fig. 2 Geometric details of the subsonic transport model (dimensions in cm).

on a lightbeam strip-chart recorder. The rolling moment was sampled for sufficient time (1 min) to ensure obtaining the maximum value at a given tunnel location. This procedure was repeated at numerous lateral and vertical positions. Figure 3 shows a typical record of rolling-moment variation with time. The source of the unsteadiness of the rolling moment signals is the meander of the vortices in the wind tunnel due to wind tunnel turbulence. Earlier studies have shown[3] that single vortices can move as much as 1 m (3.1ft). The peak rolling moment values shown in Fig. 3 are interpreted as corresponding to the times when the trailing wing is aligned with a vortex center. During the 38 sec of data shown, the peak rolling moment occurred three times.

The generator model was tested in both upright and inverted (Fig. 1) positions to evaluate strut interference effects. For the configurations with the span loading shifted inboard, in which vortices are shed inboard of the wing tip, an inverted

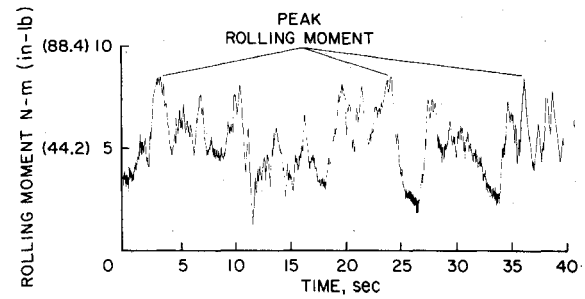

Fig. 3 Typical record of rolling moment induced on following model 1 as a function of time; generator flaps: *Ldg/Ldg*.

mounting of the generator model was required to avoid interference caused by the wake of the model mounting strut.

Flow Visualization

Wind Tunnel

The form and motion of the vortices in the wake of several configurations of the subsonic transport model were observed by the use of smoke (i.e., a vaporized oil mist) and a light slit that produced a sheet of light normal to the wake. The smoke generator apparatus and its supports were removed before rolling moment measurements were made.

Water Tow Facility

Flow visualization studies were also conducted by underwater towing of an identical generator model scaled to a 0.61-m (2-ft) span. This facility (located at the University of California's Richmond Field Station) allows flow visualization to greater downstream distances than are possible in the wind tunnel. The water tank dimensions are 1.8×2.4 m (6×8 ft) and is 61 m (200 ft) long. Tow velocities of up to 2 m/sec (6.6 ft/sec) were used. Dye was emitted at the wing tips as well as the inboard and outboard edges of the trailing edge flaps, and the light slit apparatus was again used to identify the wake structure.

Results and Discussion

Flow Visualization

The wake of the conventional flap configuration (*Ldg/Ldg*)[¶] was first observed as a basis for comparison. Figure 4a shows a photograph taken in the wind tunnel at 6

[¶]This notation means inboard flap set to the landing setting and the outboard flap set to the landing setting. See Fig. 2.

Table 1 Model dimensions and wind-tunnel conditions

Model dimensions		
Following model	1	2
Span, cm(in.)	87.4 (34.4)	33.3 (13.1)
Chord, cm(in.)	9.8 (3.9)	6.1 (2.4)
Aspect ratio	8.9	5.5
Wing section	NACA 0012	NACA 0012
Fuselage diameter, cm (in.)	5.1 (2.0)	5.1 (2.0)
Balance full-scale range, N-m (in.-lb)	11.3 (100)	3.4(30)
Generator model		
Wing		
Span, cm (in.)	179 (70.5)	
Root incidence	+2°	
Tip incidence	−2°	
Area, m^2 (ft^2)	0.459 (4.94)	
Average chord, cm (in.)	25.6 (10.1)	
Aspect ratio	7	
Horizontal stabilizer	0°	
Wind-tunnel conditions		
U_∞, m/s (fps)	40(131)	
Reynolds number based on average chord	7×10^5	

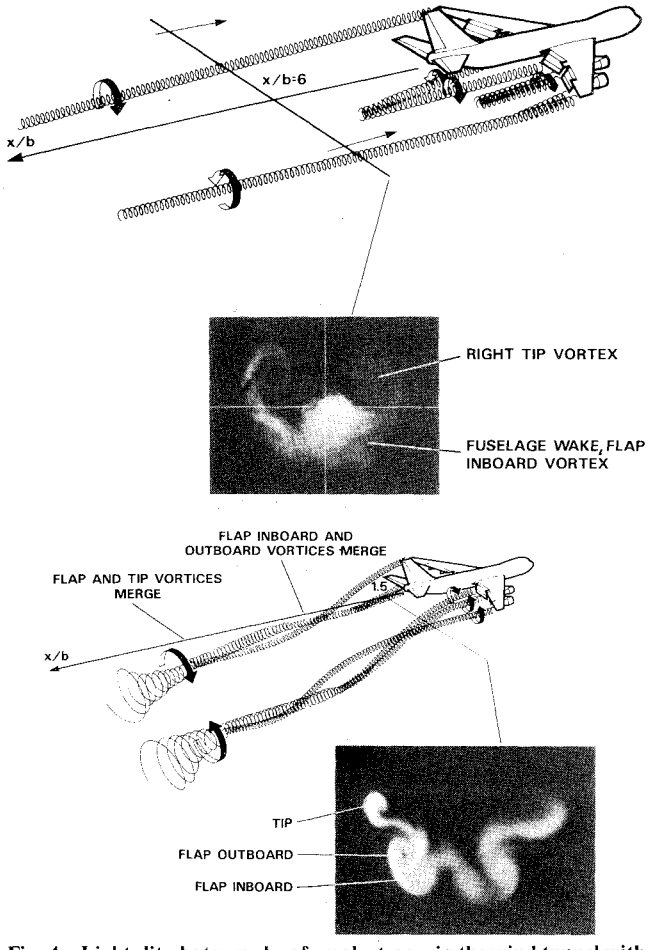

Fig. 4 Light slit photographs of smoke traces in the wind tunnel with an interpretive sketch of the wake at $U_\infty = 12$m/s (39 fps) and $C_{L_G} \approx 1.2$. a) Generator flaps: Ldg/Ldg. b) Generator flaps: $Ldg/0°$.

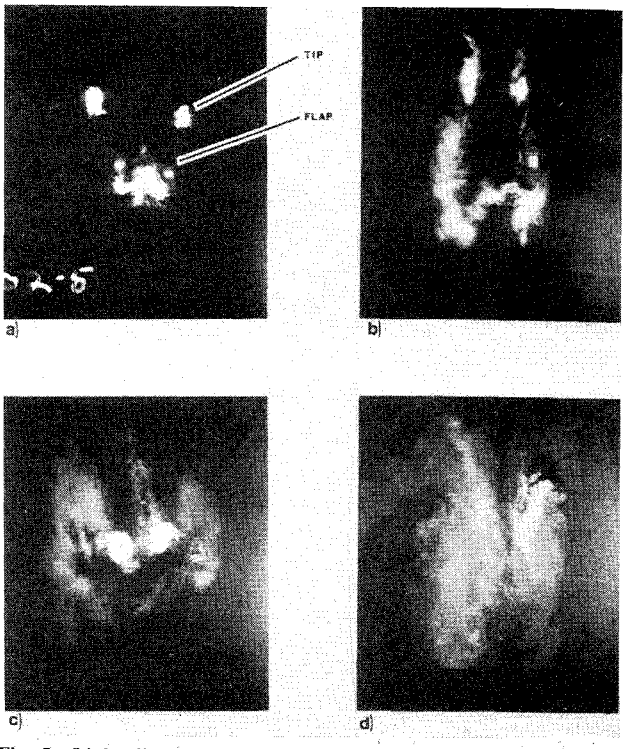

Fig. 5 Light slit photographs of dye traces in the water tow facility, generator flaps: $Ldg/0°$, $\alpha_g = 5.8°$, $U_\infty = 1$ m/sec (3.1 fps). a) $x/b_g = 1.5$. b) $x/b_g = 6$. c) $x/b_g = 13$. d) $x/b_g = 32$.

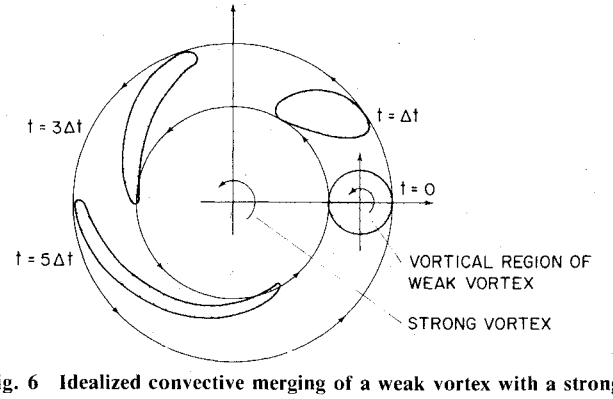

Fig. 6 Idealized convective merging of a weak vortex with a strong one.

spans downstream and a schematic of the vortex wake. This wake showed a classical arrangement consisting of two concentrated vortex cores connected by a feeding sheet at downstream distances greater than one span. At closer range a vortex pair was visible leaving the region between the inboard and outboard flap on each side of the wing, but this pair quickly diffused. Also, two vortices of like sign were seen leaving the tip region. These quickly merged into the one persisting vortex.

With the outboard flap retracted ($Ldg/0°$), the resulting wake was clearly different from the first configuration studied. Three vortices per side (Fig. 4b) rotated about one another as they moved downstream. The flap vortex and the tip vortex were initially diffuse and barely detectable by 13 spans downstream. The flap vortex and the tip vortex ultimately merged. The coalescence of the wing-tip vortex and the flap vortex was first noted by Dunham[14] in his water tank studies. This merging was clearly seen in the present water tow facility but was beyond the available viewing length in the wind tunnel. Figure 5 shows photographs taken in the present water tow facility at the same downstream stations that were used in the wind tunnel as well as at a downstream distance of 32 spans. Beyond $x/b_g = 13$, the wing-tip vortices are seen to continue to rotate an additional 90° around the flap vortices before merging with the flap vortices to become a large, diffuse rotating mass of dye, as can be seen in the photograph at $x/b_g = 32$.

The details of the merging process are not fully understood at present. However, the photographs show that merging appears to greatly accelerate the dispersion of vorticity. It was generally observed, for example, that a single vortex pair in isolation, as found with the Ldg/Ldg flap configuration, persisted for at least 40 span lengths downstream. In contrast, a wake would disperse rapidly when 1) multiple vortex pairs were shed with initially large spacing, and 2) the self-induced velocities convected these vortices into close proximity of one another. Figure 5 shows that the wing-tip and flap vortices are convected into close proximity between $x/b_g = 1.5$ and $x/b_g = 13$. The vorticity of the weak vortex (tip) is convected into an annulus around the strong vortex (flap). The mechanism of this convection is sketched schematically in Fig. 6. The vortical region of the weak vortex is taken to be circular at time zero. In the time increments shown, the region is distorted due to the velocity field of the strong vortex. When the two vortices are of comparable strength, the elongation of the core region occurs in both vortices. Additional flow visualization studies of vortex interactions have been performed by Ciffone et al.[15] The pairing of vortices of like sign has been studied by Winant et al.[16] in connection with the instability of a shear layer. They found that in the third stage of mixing layer growth, vortex pairs interacted by rolling around one another to form a single vortex in a manner that is similar to the interactions seen in the present studies. Donaldson et

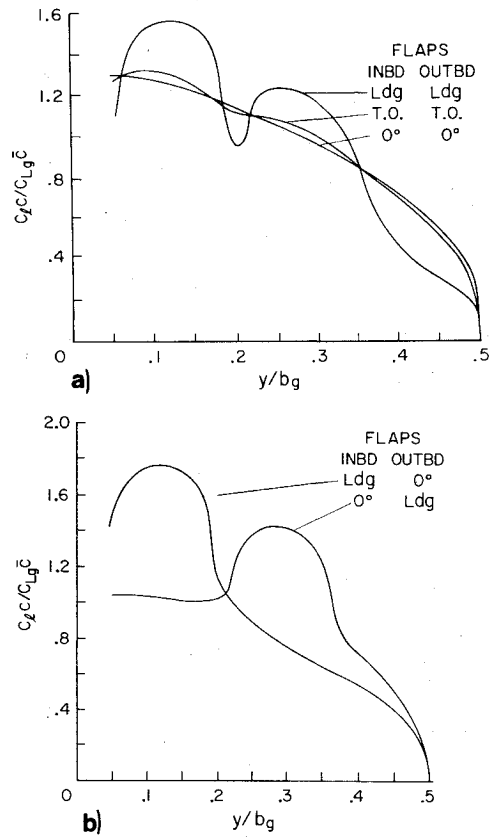

Fig. 7 Predicted span loadings on the subsonic transport model for several flap settings. a) Conventional configurations. b) Modified configuration.

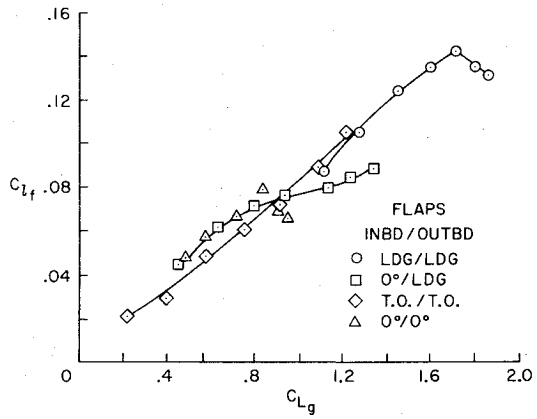

Fig. 8 Variation of peak rolling moment coefficient on following model 1 as a function of lift coefficient on the subsonic transport model for the conventional and outboard-loaded configurations, $b_f/b_g = 0.5$.

al.[17] recently calculated the interaction of two vortices using his second-order closure theory. He concluded that the turbulent kinetic energy increases substantially as a result of the interaction of the two vortices.

Span loadings computed from vortex lattice theory for the wings and flaps (including the effects of camber and twist, but without fuselage or tail) were used to indicate locations along the wing trailing edge where vortices might be expected (Fig. 7). The flaps 0° and take-off configuration span loadings are found to be approximately elliptical. Hence, these configurations shed single vortices from each wing tip.[7] With one flap retracted, the gradients in span loading are very pronounced and three vortices are shed from each wing.

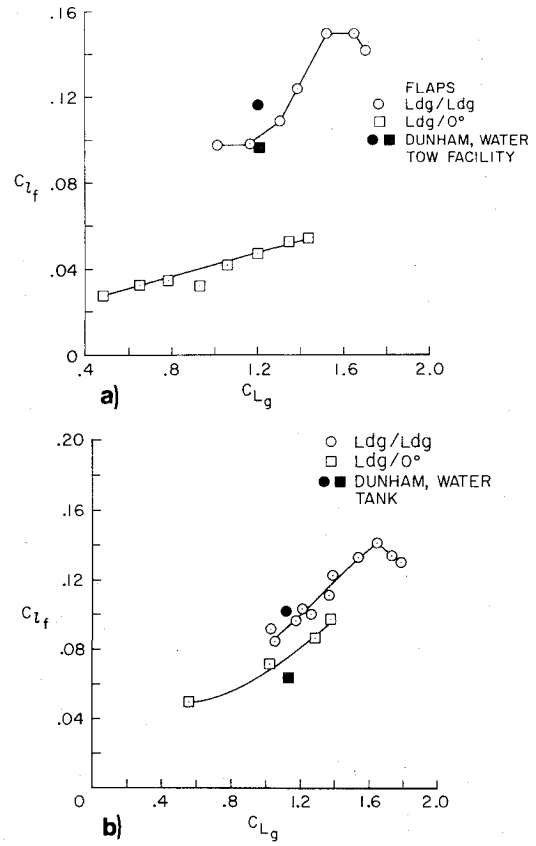

Fig. 9 Effect of inboard loading on the variation of peak rolling moment coefficient on the following model as a function of lift coefficient on the subsonic transport model. a) Following model 2, $b_f/b_g = 0.2$. b) Following model 1, $b_f/b_g = 0.5$.

Rolling-Moment Measurements

The rolling moments imposed on both trailing wings for various generating model configurations are presented in Figs. 8 and 9 as a function of the lift coefficient on the subsonic transport model. For conventional flap configurations, rolling moment on the following model increased nearly linearly with C_{L_g} up to the beginning of stall on the generator. This result is expected because the shape of the span load distribution is nearly independent of lift over the range of C_{L_g} tested, and only the magnitude changes with angle of attack. Since the vortex structure depends directly on the span loading,[7] only the total vortex strength changes with C_{L_g} thereby yielding a nearly linear relationship between C_{L_g} and C_{l_f}. Note in Fig. 8 that the various curves for the conventional configurations lie on approximately the same line. This implies that there is no major change in the vortex structure among the conventional flap configurations. An unconventional flap deflection (0°/*Ldg*) that did not yield a reduction in rolling moment also appears in Fig. 8. Below $C_{L_g} = 1.0$ these data also lie on the same line as the conventional configurations. The change in slope of the C_{l_f} curve above $C_{L_g} = 1.0$ is again associated with wing-tip stall on the generator. It is believed that this outboard loaded configuration was ineffective in reducing C_{l_f} because the wing-tip vortex and the flap outboard vortex are so close to one another that they merged with little dispersion, resulting in an intense combined vortex.

The *Ldg*/0° configuration, in contrast, produced a substantial reduction in the rolling moment on the smaller trailing wing (Fig. 9 a) and a modest reduction on the larger trailing wing (Fig. 9 b). Dunham's data,[14] taken at 14 spans, is seen to be in agreement with the present measurements for the *Ldg*/*Ldg* configuration but not for the *Ldg*/0° configuration.

However, at 30 spans downstream and beyond, his water tow data for C_{l_f} is 50% of the *Ldg/Ldg* configuration. The difference between the two results is believed to be associated with test conditions (near the generator) which lead to variations in the time required for the wake to disperse.

Flight Test Results

The favorable wind-tunnel results are also in qualitative agreement with recent flight test results[18,19] conducted by NASA as a consequence of these ground-base experiments. The flight experiments were made with a full-scale B747 airplane which could be flown with the flap configurations discussed here. Both a Lear jet and a T37 aircraft were used to probe the vortices of the generator. These aircraft have about the same span relative to the B747 as the smaller of the trailing wings in the present paper. The pilots of the probe aircraft reported that, from 4.8 to 8.0 km (3 to 5 mi) behind the trailing vortices, which were marked by smoke, appeared far more concentrated and well-defined for the *Ldg/Ldg* configuration as compared to *Ldg/0°*. Furthermore, as a result of flying in the wake at various ranges, they identified a separation requirement which was much greater for the *Ldg/Ldg* configuration than for the *Ldg/0°* configuration. An additional result (which had not been investigated in the ground-based facilities) was obtained in the flight test. It was found that, when either the landing gear of the generator was deployed or the generator was flown with yaw, a substantial part of the benefit of retracting the outboard flap was lost. An explanation for the effect of gear and yaw on the wake structure is now being studied in ground-based facilities. The details of these studies along with studies of an alternate configuration that appears to avoid the landing gear interference is contained in Refs. 15 and 20.

Rolling Moment Prediction

The method used to calculate rolling moment in the present paper is a combination of those described by Rossow et al.[21] That is, the structure of the vortex wake and the rolling moment were estimated by completing the following steps:

1. Calculate the span loading on the generating wing from vortex lattice theory.
2. Calculate the vorticity distribution at the wing trailing edge by assuming a flat wake.
3. Approximate this vorticity distribution by an array of point vortices and compute the wake rollup to $x/b_g = 3$, using an inviscid, time-dependent, two-dimensional calculation.

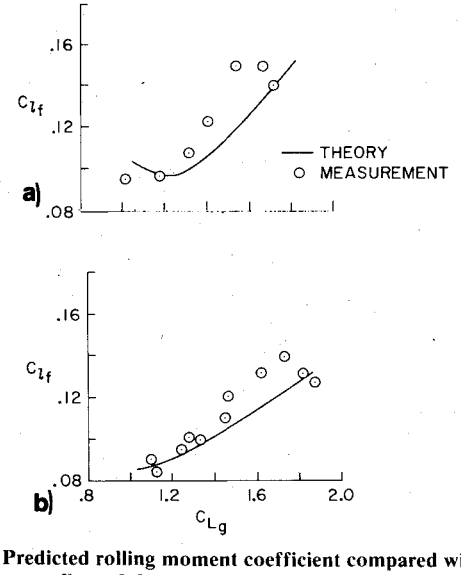

Fig. 10 Predicted rolling moment coefficient compared with present measurements; flaps: *Ldg/Ldg*. a) $b_f/b_g = 0.2$. b) $b_f/b_g = 0.5$.

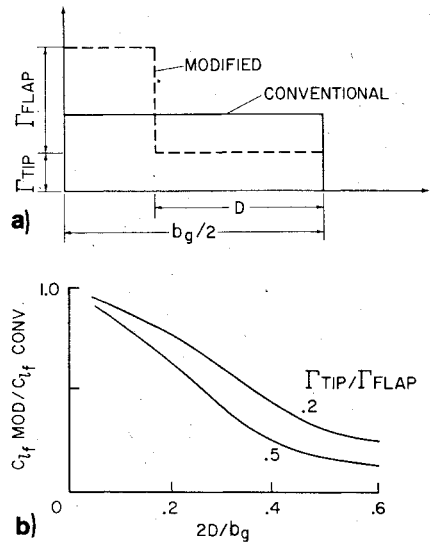

Fig. 11 Idealized example of the effect of the merging of two vortices into a single Rankine vortex on the rolling moment coefficient on a follower as compared to a single vortex wake at the same lift and span, $b_f/b_g = 0.2$. a) Span loading. b) Rolling moment ratio.

4. At $x/b_g = 3$, group point vortices to yield a radial distribution of circulation about each vortex center.
5. Finally, calculate the rolling moment on the following wing using strip theory[12] for each of the vortex groups.

Comparison of Results

The foregoing steps were used to calculate the rolling moment on the two trailing wings for a range of angle of attack of the generating model when its flaps were deflected to the *Ldg/Ldg* configuration. The curves shown in Figs. 10a and 10b are the computed rolling-moment coefficient when the centerline of the trailing wing coincides with the centroid of vorticity. The theoretical curves are in good agreement with the experimental data.

As noted in the flow visualization, the wing-tip and flap vortices for the *Ldg/0°* configuration merged. Unfortunately, the preceding theoretical method was incapable of predicting this merger for sufficient distance downstream of the generator. The predicted C_{l_f} for the fully merged case would be expected, however, to be substantially below that for the conventional configuration. This is illustrated in the following section.

Merging of Two Vortices

Consider the two idealized span loadings sketched in Fig. 11 a. For the modified configuration, the wing-tip and flap vortices are assumed to merge into the single circular vortex core with uniformly distributed vorticity (i.e., Rankine vortex). The circulation and core diameter of this merged vortex was obtained from the vortex invariants attributed to Betz and discussed by Rossow.[7] The rolling-moment coefficent on the follower in the wake of this merged vortex, as well as in the wake of the single vortex of the conventional configuration, was computed according to step 5 in the preceding. This result is shown on Fig. 11b as a function of the spacing between the two vortices of the modified configuration. As shown, for vortex spacing in excess of 0.3 of the semispan, the reduction in rolling-moment coefficient behind the modified configuration, as compared with the conventional configuration, is substantial. The values of $2D/b_g$ of interest are those sufficiently small that merger occurs within a useful downstream distance. If $2D/b_g$ is too large, the flap vortex will move away from the wing-tip vortex under the influence of the flap vortex from the other side of the wing, thereby delaying or eliminating a merger.

This example illustrates that the measured reduction in rolling moment on a follower can be substantially accounted for on the basis of inviscid effects alone. Viscous diffusion of the trailing vortex will further reduce the rolling moment on the follower. The actual relative contribution of viscous and inviscid effects is not known.

Conclusions

Previous studies of the effect of span loading on wake vortex structure indicated that dispersion of the lift-generated vorticity could be accelerated by modifying the conventional spanwise loadings. The present investigation showed that deflecting only the inboard flaps so that three vortex pairs were shed by the wing was effective in dispersing wake vorticity. This resulted in reduced rolling moments imposed on wings encountering this wake. Flow visualization indicated that these vortices ultimately merged into one large, diffuse vortex per side. The merging mechanism discussed here suggests that the reduction in rolling moment is attributable to the merger of multiple vortices that are initially separated from one another by a sizable fraction on the semispan of the generator.

References

[1]Patterson, J.C.,"Lift-Induced Wing-Tip Vortex Attenuation," *Journal of Aircraft,* Vol. 12, Sept. 1975, pp. 745-749.

[2]Corsiglia, V.R., Jacobsen, R.A., and Chigier, N., "An Experimental Investigation of Trailing Vortices Behind a Wing with a Vortex Dissipator," *Aircraft Wake Turbulence,* Edited by John H. Olsen, Arnold Goldberg, and Milton Rogers, Plenum Publishing Corp., New York, Sept. 1970.

[3]Corsiglia, V.R., Schwind, R.K., and Chigier, N.A., "Rapid-Scanning, Three-Dimensional Hot-Wire Anemometer Surveys of Wing-Tip Vortices," *Journal of Aircraft,* Vol. 10, Dec. 1973, pp. 752-757.

[4]Croom, D., "Low-Speed Wind-Tunnel Investigation of Forward-Located Spoilers and Trailing Splines as Trailing-Vortex Hazard-Alleviation Devices on an Aspect-Ratio-8 Wing Model," NASA TM - 3166, Feb. 1975.

[5]Bilanin, A.J. and Widnall, S.E., "Aircraft Wake Dissipation by Sinusoidal Instability and Vortex Breakdown," AIAA Paper 73-107, Washington, D.C., 1973.

[6]Chevalier, H., "Flight Test Studies of the Formation and Dissipation of Trailing Vortices," *Journal of Aircraft,* Vol. 10, Jan. 1973 pp. 14-18.

[7]Rossow, V.J., "On the Inviscid Rolled-Up Structure of Lift-Generated Vortices," *Journal of Aircraft,* Vol. 10, Nov. 1973, pp. 647-650.

[8]Rossow, V.J., "Theoretical Study of Lift-Generated Vortex Wakes Designed to Avoid Rollup," *AIAA Journal,* Vol. 13, April 1975, pp. 476-484.

[9]Ciffone, D.L. and Orloff, K.L., "Far-Field Wake-Vortex Characteristics of Wings," *Journal of Aircraft,* Vol. 12, May 1975, pp. 464-470.

[10]Wentz, W.H., Jr., "Evaluation of Several Vortex Dissipators by Wind Tunnel Measurements of Vortex-Induced Upset Loads," Wichita State Univ. Aeronautical Rept. 72-3, Sept. 1972.

[11]Singh, B., Kutty, T.M., and Wentz, W.H., Jr., "Preliminary Investigation of Rolling Moments Induced by Trailing Vortices for Several Wing-Tip Modifications," Wichita State Univ. Aeronautical Rept. 72-1, Jan. 1972.

[12]Banta, A.J., "Effects of Planform and Mass Injectin on Rolling Moments Induced by Trailing Vortices," Master's Thesis, Wichita State Univ., Wichita, Kansas, Dec. 1973.

[13]Iversen, J.D. and Bernstein, S., "Trailing Vortex Effects on Following Aircraft," *Journal of Aircraft,* Vol. 11, Jan. 1974, pp. 60-61.

[14]Dunham, E.R., Jr., "Model Tests of Various Vortex Dissipation Techniques in a Water Towing Tank," NASA TN (to be published).

[15]Ciffone, D.L. and Lonzo, C., Jr., "Flow Visualization of Vortex Interactions in Multiple Vortex Wakes Behind Aircraft," NASA TM X-62,459, June 1975.

[16]Winant, C.D. and Browand, F.K., "Vortex Pairing: The Mechanisims of Turbulent Mixing Layer Growth at Moderate Reynolds Number," *Journal of Fluid Mechanics,* Vol. 63, Part 2, 1974, pp. 237-255.

[17]Donaldson, C. and Bilanin, A., "Vortex Wakes of Conventional Aircraft." AGARD-AG204, May 1975.

[18]Tymczyszyn, J. and Barber, M.R., "A Review of Recent Wake Vortex Flight Tests," 18th Annual Symposium of Society of Experimental Test Pilots, Los Angeles, Calif., Sept. 26, 1974.

[19]Smith, H.J., "A Flight Test Investigation of the Rolling Moments Induced on a T-37B Airplane in the Wake of a B-747 Airplane," NASA TM X-56,031, April 1975.

[20]Corsiglia, V.R. and Dunham, R.E., "Aircraft Wake-Vortex Minimization By Use of Flaps," Proceeding from NASA Symposium on Wake Vortex Minimization, Washington, D.C., Feb. 25-26, 1976.

[21]Rossow, V.J., Corsiglia, V.R., Schwind, R.G., Frick, J.K.D., and Lemmer, O.J., "Velocity and Rolling-Moment Measurements in the Wake of a Swept Wing Model in the 40-by 80-Foot Wind Tunnel," NASA TM X-62,414, April 1975.